

University of Windsor

## Scholarship at UWindsor

---

Chemistry and Biochemistry Publications

Department of Chemistry and Biochemistry

---

2022

### Influence of ceramide on lipid domain stability studied with small-angle neutron scattering: The role of acyl chain length and unsaturation

Mitchell Dipasquale  
*University of Windsor*

Tye G. Deering  
*University of Virginia*

Dhimant Desai  
*Pennsylvania State University*

Arun K. Sharma  
*Pennsylvania State University*

Shantu Amin  
*Pennsylvania State University*

Follow this and additional works at: <https://scholar.uwindsor.ca/chemistrybiochemistrypub>

See next page for additional authors

 Part of the [Biochemistry, Biophysics, and Structural Biology Commons](#), and the [Chemistry Commons](#)

---

#### Recommended Citation

Dipasquale, Mitchell; Deering, Tye G.; Desai, Dhimant; Sharma, Arun K.; Amin, Shantu; Fox, Todd E.; Kester, Mark; Katsaras, John; Marquardt, Drew; and Heberle, Frederick A.. (2022). Influence of ceramide on lipid domain stability studied with small-angle neutron scattering: The role of acyl chain length and unsaturation.

<https://scholar.uwindsor.ca/chemistrybiochemistrypub/329>

This Article is brought to you for free and open access by the Department of Chemistry and Biochemistry at Scholarship at UWindsor. It has been accepted for inclusion in Chemistry and Biochemistry Publications by an authorized administrator of Scholarship at UWindsor. For more information, please contact [scholarship@uwindsor.ca](mailto:scholarship@uwindsor.ca).

---

**Authors**

Mitchell Dipasquale, Tye G. Deering, Dhimant Desai, Arun K. Sharma, Shantu Amin, Todd E. Fox, Mark Kester, John Katsaras, Drew Marquardt, and Frederick A. Heberle

# **Influence of ceramide on lipid domain stability studied with small-angle neutron scattering: The role of acyl chain length and unsaturation**

Mitchell DiPasquale,<sup>†</sup> Tye G. Deering,<sup>‡</sup> Dhimant Desai,<sup>¶</sup> Arun K. Sharma,<sup>¶</sup>  
Shantu Amin,<sup>¶</sup> Todd E. Fox,<sup>‡</sup> Mark Kester,<sup>‡,§</sup> John Katsaras,<sup>\*,||,⊥,#</sup> Drew  
Marquardt,<sup>\*,†,@</sup> and Frederick A. Heberle<sup>\*,△</sup>

<sup>†</sup>*Department of Chemistry and Biochemistry, University of Windsor, Windsor, ON,  
Canada*

<sup>‡</sup>*Department of Pharmacology, University of Virginia, Charlottesville, VA 22908, USA*

<sup>¶</sup>*Department of Pharmacology, Penn State University, State College, PA 16801, USA*

<sup>§</sup>*Department of Molecular Physiology and Biophysics, University of Virginia,  
Charlottesville, VA 22908, USA*

<sup>||</sup>*Neutron Scattering Division, Oak Ridge National Laboratory, Oak Ridge, TN, 37831, USA*

<sup>⊥</sup>*Joint Institute for Neutron Sciences, Oak Ridge National Laboratory, Oak Ridge, TN  
37831, USA*

<sup>#</sup>*Department of Physics and Astronomy, University of Tennessee, Knoxville, TN 37996,  
USA*

<sup>@</sup>*Department of Physics, University of Windsor, Windsor, ON, Canada*

<sup>△</sup>*Department of Chemistry, University of Tennessee, Knoxville, TN 37996, USA*

E-mail: katsarasj@ornl.gov; drew.marquardt@uwindsor.ca; fheberle@utk.edu

## Abstract

Ceramides and diacylglycerols are groups of lipids capable of nucleating and stabilizing ordered lipid domains, structures that have been implicated in a range of biological processes. Previous studies have used fluorescence reporter molecules to explore the influence of ceramide acyl chain structure on sphingolipid-rich ordered phases. Here, we use small-angle neutron scattering (SANS) to examine the ability of ceramides and diacylglycerols to promote lipid domain formation in the well-characterized domain-forming mixture DPPC/DOPC/cholesterol. SANS is a powerful, probe-free technique for interrogating membrane heterogeneity, as it is differentially sensitive to hydrogen's stable isotopes protium and deuterium. Specifically, neutron contrast is generated through selective deuteration of lipid species, thus enabling the detection of nanoscopic domains enriched in deuterated saturated lipids dispersed in a matrix of protiated unsaturated lipids. Using large unilamellar vesicles, we found that upon replacing 10 mol % DPPC with either C16:0 or C18:0 ceramide, or 16:0 diacylglycerol (dag), lipid domains persisted to higher temperatures. However, when DPPC was replaced with short chain (C6:0 or C12:0) or very long chain (C24:0) ceramides, or ceramides with unsaturated acyl chains of any length (C6:1(3), C6:1(5), C18:1, and C24:1), as well as C18:1-dag, lipid domains were destabilized, melting at lower temperatures than those in the DPPC/DOPC/cholesterol system. These results show how ceramide acyl chain length and unsaturation influence lipid domains, and have implications for how cell membranes might modify their function through the generation of different ceramide species.

## Introduction

The liquid-ordered (Lo) membrane phase is a unique state of matter that arises from a preferential interaction between cholesterol and either sphingolipids or saturated phospholipids.<sup>1</sup> In the presence of unsaturated phospholipids, Lo phases can coexist with disordered liquid (Ld) phases over a broad range of composition and temperature.<sup>2,3</sup> The appearance

of Ld+Lo phase separation in model membranes that mimic the composition of eukaryotic plasma membrane outer leaflet has generally helped shed light on observations of lipid rafts in living cells.<sup>4</sup> In particular, rafts are thought to be ordered lipid domains enriched in cholesterol and sphingolipids that are stabilized by a network of hydrogen bonds.<sup>5,6</sup> The small (nanoscopic) size and transient lifetime of ordered domains in resting cells has fueled an ongoing debate regarding the physicochemical origins of membrane rafts.<sup>7</sup> Whether these domains are a manifestation of Ld+Lo phase separation,<sup>8</sup> critical fluctuations,<sup>9</sup> a microemulsion,<sup>10</sup> or some other mechanism remains an open question.

Although the canonical raft models are understandably based on the most abundant classes of plasma membrane lipids (i.e., ternary mixtures of high-melting and low-melting phospholipids together with cholesterol), minor plasma membrane lipid components can have a profound influence on raft behavior. A prime example are ceramides, a diverse class of sphingolipid metabolites that are among the most hydrophobic biomolecules found in nature.<sup>11</sup> Similarly to cholesterol, ceramides can selectively partition into ordered lipid phases to minimize their interaction with water.<sup>12,13</sup> As shown in Figure 1A, the relatively small hydroxyl headgroup of ceramide, together with its sphingoid backbone and long acyl chains, produce a structure that is highly suited for interactions with ordered lipid domains. Under certain conditions, ceramides can reach concentrations of up to 10 mol % in ordered phases<sup>14</sup> and may have a greater propensity than cholesterol to associate with ordered phases.<sup>12,15</sup> The association between ceramides and ordered lipid phases is known to stabilize lipid domains,<sup>16</sup> but in turn excludes cholesterol from these domains.<sup>17,18</sup>

The complex interaction between ceramide, cholesterol, and other raft-forming lipids is becoming a topic of increasing interest, as an understanding of their physicochemical properties is of central importance for defining the potential biological roles of lipid rafts.<sup>19,20</sup> For example, ceramides have been shown to participate in a wide range of cellular processes taking place at the membrane, including protein function,<sup>11</sup> signalling,<sup>21,22</sup> and apoptosis.<sup>23-25</sup> Moreover, the differential tissue expression of various ceramide synthases points to different

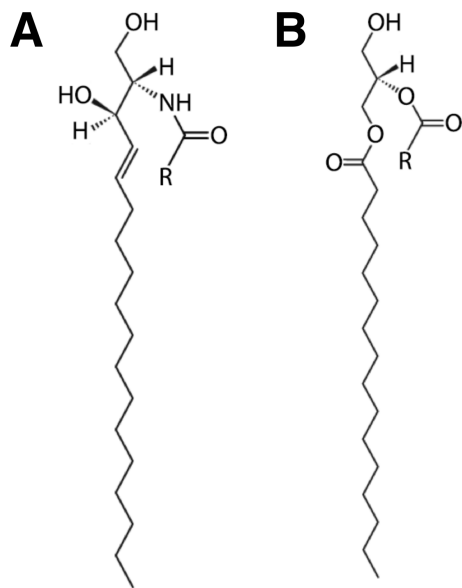


Figure 1: Structures of (A) ceramide (cer) and (B) diacylglycerol (dag). In contrast to the glycerol backbone of phospholipids, the sphingoid backbone of ceramide is both a hydrogen bond donor and acceptor.

membrane behaviors associated with particular ceramide acyl chains.<sup>26</sup>

Several studies have found that ceramides can displace cholesterol from sphingolipid-rich ordered phases, essentially modifying membrane fluidity by forming ceramide-rich gel domains.<sup>27-30</sup> In most of these studies, lipid phase behavior was interrogated through the use of fluorescent reporter molecules, which can in some cases perturb the local membrane environment.<sup>31</sup> In this work, we used small-angle neutron scattering (SANS), an essentially probe-free technique capable of detecting nanoscopic lipid domains.<sup>32,33</sup> Specifically, we used SANS to report on the clustering of saturated lipids in the presence of different ceramide and diacylglycerol species. Diacylglycerols (Fig. 1B) are structurally similar to ceramides but lack the ability to hydrogen bond. We chose a glycerophospholipid-based lipid composition to reduce backbone hydrogen bonding, thus allowing us to better compare the effects of ceramide and diacylglycerol acyl chains. Our experimental strategy was to replace 10 mol % of the saturated lipid in the prototypical ternary domain-forming composition DPPC/DOPC/Chol (37.5/37.5/25) with various species of ceramide or diacylglycerol dif-

fering in fatty acid chain length and degree of unsaturation, resulting in a quaternary mixture with sufficient amounts of saturated lipid and cholesterol to inhibit the formation of ceramide-rich gel domains.<sup>34-37</sup>

## Results

We collected SANS data for extruded large unilamellar vesicle (LUV) samples in which the average neutron scattering length density (NSLD) of the lipid bilayer was matched to the surrounding water, but where the average NSLDs of the saturated and unsaturated lipid species were not matched to each other. In such a sample, any excess coherent scattering above the flat incoherent background is the result of a nonrandom lateral spatial arrangement of saturated and unsaturated lipids (i.e., lipid clustering) on length scales accessible to the SANS technique (i.e., domains of greater than  $\approx 5$  nm).<sup>33</sup> We compared samples doped with protiated ceramide (cer) or diacylglycerol (dag) species to a baseline mixture devoid of the dopant. The baseline composition was DPPC/DOPC/Chol (37.5/37.5/25, by mole fraction), a well-characterized mixture that phase-separates into coexisting liquid-ordered (saturated-rich,  $L_o$ ) and liquid-disordered (unsaturated-rich,  $L_d$ ) domains below  $\approx 32$  °C.<sup>34</sup> In each sample, 10 mol % of the saturated lipid DPPC was replaced by a cer or dag of different acyl chain length and/or degree of unsaturation, while keeping the overall average NSLD of the mixture constant.<sup>33</sup> Using this experimental approach, we maintained a constant molar ratio of cholesterol, cer/dag, and high-melting temperature lipid, which has been shown to be a critical modulator of phase behaviour in ceramide containing mixtures.<sup>36-38</sup> The use of DPPC (rather than sphingomyelin) in the baseline mixture avoids bias toward domain stabilization by hydrogen bonding between the sphingoid backbone of ceramide and that of sphingomyelin lipids.<sup>27,39</sup>

Previous work using a sphingolipid-based, raft-forming ternary mixture suggested that some ceramides with long acyl chains can form a ceramide-rich gel ( $L_\beta$ ) phase at low cholest-

terol concentrations.<sup>36</sup> We used a cholesterol concentration (25 mol %) that is significantly higher than the ceramide concentration (10 mol %) to minimize the possibility of  $L_{\beta}$  formation. Additionally, because the ceramide and diacylglycerol species are protiated, any induced gel domains would have an NSLD similar to the protiated bulk phase, and thus changes in scattering can be directly correlated to changes in the clustering of deuterated DPPC-rich  $L_0$  phase.

Figure 2 shows SANS curves for the ceramide-free baseline sample as well as samples where 10 mol % of the DPPC was replaced by either C18:0-cer or C18:1-cer. At 15 °C, the ceramide-free sample (blue curve) shows a characteristic peak at  $\approx 0.005 \text{ \AA}^{-1}$  resulting from lateral segregation of the deuterated and protiated lipid components, consistent with previous observations.<sup>40</sup> The coherent scattering peak is markedly reduced upon raising the temperature to 25 °C, and is completely lost by 35 °C, suggesting a well-mixed fluid bilayer, consistent with published phase diagrams for this mixture.<sup>34</sup> Partial replacement of DPPC with C18:0-cer (orange curve) increases the scattering intensity relative to the baseline mixture at all temperatures, indicating that this lipid induces greater segregation of DPPC from the other lipids. In contrast, C18:1-cer (red curve) abolishes coherent scattering at all temperatures, suggesting that this lipid causes DPPC to mix with the other lipids.

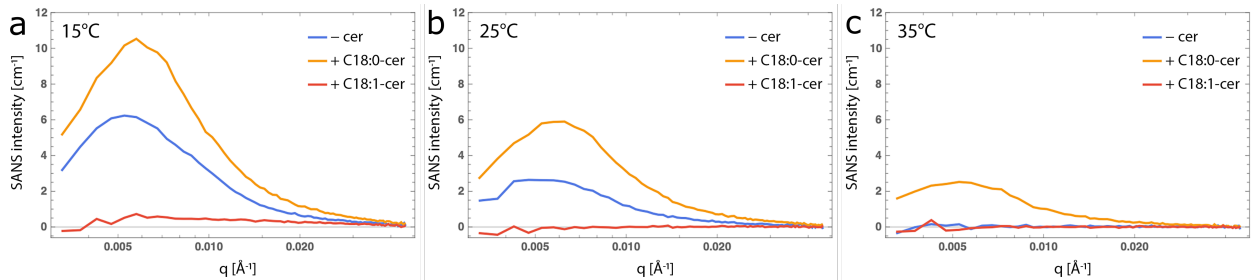


**Figure 2: SANS reveals the effects of membrane additives on domain stability.** SANS data at 15 °C (a), 25 °C (b), and 35 °C (c) for the lipid mixture DPPC/DOPC/Chol 37.5/37.5/25 in the absence of ceramide (-cer, blue curve), or with 10 mol % of DPPC replaced by either C18:0-cer (orange curve), or C18:1-cer (red curve). C18:0-cer stabilizes domains as indicated by an increase in SANS intensity relative to the baseline, while C18:1-cer destabilizes domains. Close to physiological temperature (c), C18:0-cer induces domain formation in the uniform baseline lipid mixture.



To quantitatively compare the influence of the different ceramide species on lateral lipid heterogeneity, we calculated the Porod invariant,  $Q$ , from the SANS data as described in the Experimental Procedures. Given the contrast scheme, an increase (decrease) in  $Q$  reflects stronger (weaker) lateral segregation of saturated and unsaturated lipids, that is, a change in the propensity of the ordered lipid DPPC to cluster. Here and throughout, we use the shorthand language that increased  $Q$  corresponds to a dopant that stabilizes domains, while decreased  $Q$  corresponds to domain destabilization. Figure 3 shows  $Q$  plotted against acyl chain length for various saturated and unsaturated (open circles and triangles, respectively) ceramides and diacylglycerols (blue and orange symbols, respectively) at (a) 15 °C, (b) 25 °C, and (c) 35 °C. Of the eleven species investigated, only three (i.e., C16:0-cer, C18:0-cer, and C16:0-dag) were found to stabilize domains and, as shown in Fig. 3c, induce domains in an otherwise uniform mixture at 35 °C. In contrast, domains were destabilized by dopants with short saturated chains (C6:0-cer and C12:0-cer), long saturated chains (C24:0-cer), or by an unsaturated chain of any length (C6:1-cer, C18:1-cer, C24:1-cer, and C18:1-dag).

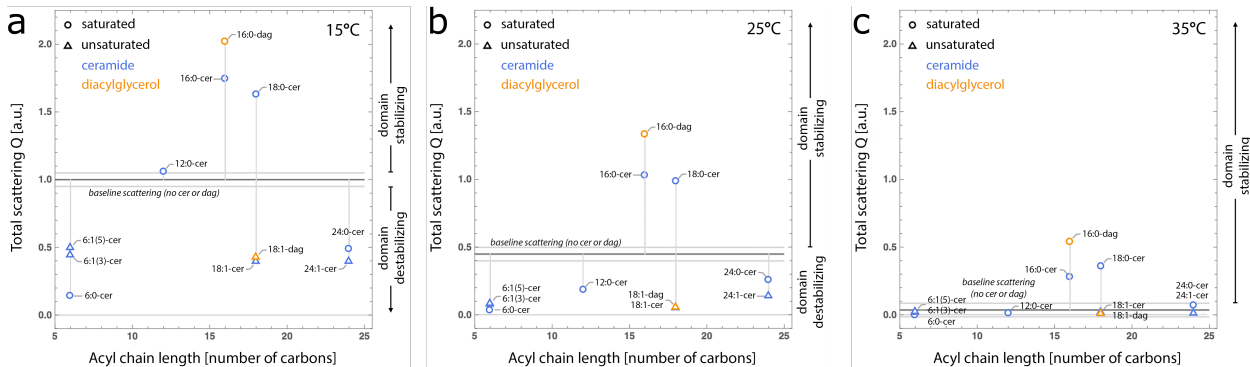


Figure 3: **Domain stabilization or destabilization by ceramide depends on the structure of its N-acyl chain.** The normalized Porod invariant,  $Q$ , is correlated to the acyl chain length of different saturated and unsaturated (open circles and open triangles, respectively) ceramides and diacylglycerols (blue and orange, respectively) at (a) 15 °C, (b) 25 °C, and (c) 35 °C. Species above the horizontal black line stabilize domains relative to the baseline lipid mixture, while those below the line destabilize domains. The horizontal gray lines denote one standard deviation derived from replicate experiments of the baseline composition.

Considering only the ceramide species, the hierarchy for propensity to stabilize domains is

as follows: C18:0  $\approx$  C16:0 > no ceramide  $\approx$  C12:0 > C24:0  $\approx$  C24:1  $\approx$  C18:1  $\approx$  C6:1 > C6:0. At all temperatures studied, C6:0-cer was found to be most strongly destabilizing to domains, even more so than its unsaturated counterpart. Comparison of chain-analogous ceramides and diacylglycerols in Fig. 3 shows a slightly greater propensity for diacylglycerol species to stabilize domains (compare e.g. C16:0-cer and C16:0-dag). However, introduction of a domain suppressing feature such as chain unsaturation negates the stabilizing contribution of the backbone (compare e.g. C18:1-cer and C18:1-dag).

## Discussion

Using a probe-free neutron scattering technique, we investigated the effect of ceramide or diacylglycerol structure on the lateral organization of phosphatidylcholine bilayers exhibiting Ld+Lo phase separation. While many studies have focused on the competition between cholesterol and ceramide in sphingomyelin-rich domains,<sup>27,36,41</sup> we used a system of glycerophospholipids to restrict hydrogen bonding contributions,<sup>5</sup> thereby emphasizing the role of the N-acyl chain. Our baseline composition presents domains with a moderate proportion of cholesterol (25 mol %).<sup>34</sup> We observe changes in DPPC clustering at low ratios of ceramide:saturated lipid, which are devoid of gel phases owing to the cholesterol content.<sup>36</sup> In agreement with previous studies, we find the following rank order of structural features that influence lateral organization: chain unsaturation > chain length > backbone structure.

### Ceramide chain unsaturation suppresses domains

All unsaturated ceramide species studied here promote the mixing of saturated and unsaturated lipid components. Structurally, the small polar headgroups of ceramides and diacylglycerols result in conical lipid shapes that destabilize lamellar phases.<sup>42</sup> Moreover, *cis*-double bonds introduce kinks in the acyl chains that further decrease molecular packing efficiency and limit van der Waals interactions between adjacent acyl chains.<sup>43</sup> Regardless,

monolayer and fluorescence studies have shown that unsaturated ceramide species favourably interact with condensed phases.<sup>12,27,28,44</sup> As a result of their molecular structures, ceramides and diacylglycerols seek out ordered domains as a means to shelter their large hydrophobic moieties from the aqueous phase, analogous to the “umbrella model” in the case of cholesterol.<sup>13</sup> We find that incorporation of cer or dag species containing chain unsaturations destabilizes domains, presumably by lowering domain order and thus reducing the difference in order between Lo and Ld phases.

Interestingly, at 15 °C (Fig. 3a) all of the unsaturated lipids that we studied appear to suppress lateral phase separation to approximately the same degree. As noted in previous work,<sup>27,28</sup> the location of the *cis*-double bond is a critical factor in determining the extent of lipid domain destabilization. As shown in Fig.3a, comparing C6:1-cer species with equivalent chain length and unsaturation, the centralized double bond of C6:1(3)-cer destabilizes domains to a greater degree than the distal double bond of C6:1(5)-cer. This trend is recapitulated in comparison of two  $\omega$ -9 fatty acid-containing ceramides, where the more centrally located double bond of C18:1-cer $^{\Delta 9c}$  abolished domains at a lower temperature than C24:1-cer $^{\Delta 15c}$  (Fig.3b).

It has previously been shown that the highly asymmetric acyl chains of C24:1-cer can induce interdigitated phases in mixed lipid membranes.<sup>45,46</sup> Interdigitation might minimize packing constraints and stabilize domains containing long unsaturated ceramide chains. At 15 °C (Fig. 3a), all unsaturated acyl chain ceramides produce vesicles with approximately 40 % of the total scattering Q of the system with no ceramide. Increasing the temperature to 25 °C (Fig. 3b) results in a lesser decrease in Q for C24:1-cer compared to the other unsaturated ceramides, suggesting a greater resistance of the C24:1-cer-containing domains to thermal disruption. Our data supports an additional contribution, such as interdigitation, as a mechanism to stabilize phases by limiting packing constraints. The effect of interdigitation is also evidenced by the greater ability of C24:1-cer to form gel domains in bilayers<sup>45</sup> compared to monolayers.<sup>44</sup>

## Ceramide chain length tunes domain stability

Earlier studies identified that trends in the membrane behavior of ceramides are correlated with the length of their N-acyl chains, and that a matched hydrophobic thickness maximizes van der Waals interactions to stabilize gel-like phases.<sup>47,48</sup> In contrast, it has also been shown that progressive chain asymmetry and mismatch of bilayer thickness decreases the miscibility transition temperature (i.e., destabilizes sterol-sphingolipid ordered domains).<sup>27,29</sup> Our results align well with existing literature in identifying C16:0-cer as the most domain stabilizing ceramide species in mixtures with where ordered phases are enriched in palmitoyl chains.<sup>27,28,30,37,49,50</sup>

Ceramides have been shown to have a greater affinity for ordered phases than does cholesterol.<sup>12,15,44</sup> For example, multiple studies have shown that matching N-acyl length ceramides (C16:0-cer and C18:0-cer) are able to efficiently out-compete cholesterol for association with ordered lipids.<sup>27,35,41,50,51</sup> Given our neutron contrast matching scheme (described in Materials and Methods), an increase in the total scattering  $Q$  can be attributed to increases in either or both of two interdependent modes: (i) a greater area fraction of ordered domains ( $a_d$ ); and (ii) greater contrast ( $\Delta\rho$ ) due to stronger partitioning of DPPC between the ordered domains and bulk disordered phase. Based on increased total scattering, our data show that these chain-matched species are most effective in promoting clustering of the saturated DPPC lipids. This stabilizing effect is very pronounced and results in the formation of ordered lipid domains in what would otherwise have been a homogeneous mixture at near-physiological temperature (Fig. 3c).

Highly asymmetric ceramide species induce disordering of saturated lipids to varying degrees. Very long-chain ceramides (C24:0-cer) possesses a strong negative curvature and the ability to interdigitate. These features can promote tubule formation at high ceramide concentrations,<sup>28,52,53</sup> though we do not observe any evidence of tubulation at 10 mol % ceramide. As a consequence of their ability to perturb molecular packing, condensed phases composed of very long-chain ceramides are less ordered and exhibit complex melting behavior.<sup>27</sup> At a 1:1

stoichiometry of saturated lipid:ceramide and 10 mol % cholesterol, Maula et al. found that C24:0-cer promotes membrane order, albeit less so compared to C16:0-cer or C18:0-cer.<sup>27</sup> In the current study, we used a higher proportion of saturated lipid and cholesterol (a saturated lipid:ceramide molar ratio of 2.75:1 and 25 mol % cholesterol) and found that C24:0-cer destabilizes saturated lipid clusters. The discrepancy between this and previous results can be rationalized by the lower capacity of POPC/PSM/Chol/Cer (60/15/10/15) to shelter ceramide from the aqueous phase, compared to DOPC/DPPC/Chol/Cer (37.5/27.5/25/10). The limited shielding capacity of the former mixture forces a closer association between the ceramide and saturated lipid. We further note that of all the lipid species we identified as destabilizing lipid domains (i.e., those beneath the horizontal line in Fig. 3), the composition with C24:0-cer was the least responsive to temperature. Although C24:0-cer decreases the ability of DPPC to cluster, the ordered phase that it forms is rather robust, possibly due to its ability to interdigitate.<sup>52</sup>

Short chain ceramides are known to have a significant disordering effect on biological membranes and are not known to induce acyl chain interdigitation. Our work closely mirrors that of Megha et al., which studied the behavior of ceramides in brain sphingomyelin and reached similar conclusions regarding the influence of short-chain ceramides on domain stability. Though that study used a larger ceramide mole fraction (18 mol %, compared to 10 mol % in the present study), the authors observed a slightly destabilizing effect on lipid rafts upon incorporation of C12:0-cer, which they attributed to the ability of the ceramide to displace cholesterol.<sup>30</sup> Additionally, Megha et al. found C6:0-cer to be among the lipids with the greatest ability to destabilize ordered lipid domains, in agreement with the work of Nybond et al. and our findings.<sup>29</sup> Domain disordering by short-chain ceramides has been suggested to arise from perturbations to interfacial lipid packing caused by the short acyl chain.<sup>29</sup> Our results show that these short chain species do not provide sufficient favourable interactions to stabilize ordered phases and thus result in significant membrane disorder, with C6:0-cer being the most domain destabilizing lipid of those studied here. Several studies have shown

that C6:0-cer is the most apoptotic ceramide species, which may be a consequence of this destabilization.<sup>54-57</sup>

Work by Megha and London suggested a limited capacity of ordered phases to accommodate small-headgroup ceramide species.<sup>15,50</sup> This solubility limit results in a competition between cholesterol and ceramide that leads to the most favorable association, i.e., a gel phase enriched in ceramide and saturated lipid.<sup>15</sup> The extent of the competition depends on the relative amounts of ceramide/cholesterol and the saturated lipid species. When the saturated lipid is in limited supply, even small amounts of ceramide are observed to displace cholesterol from ordered domains.<sup>35,36,49</sup> In biological membranes, the displaced cholesterol can be removed from the bilayer through various pathways.<sup>58</sup> However, at fixed lipid compositions such as those found in model membrane studies, cholesterol is released and is then able to nucleate a liquid-ordered phase domain.<sup>35,50</sup> Indeed, the formation of ceramide-rich gel domains surrounded by a cholesterol-rich liquid-ordered phase has been inferred from FRET and fluorescence anisotropy data.<sup>37,49,59</sup> Alternatively, at intermediate cholesterol concentrations and with an abundance of saturated lipid (such as in this work), the competition between cholesterol and ceramide results in the formation of an ordered phase composed primarily of saturated lipid, cholesterol, and ceramide.<sup>27,46,60,61</sup> This heterogeneous ordered phase may have unique physicochemical properties as it teeters between a cholesterol-rich ( $L_o$ , no long range order) and a ceramide-rich ( $L_\beta$ , long range order) phase.<sup>38,50,62,63</sup> Future studies probing the physical properties of heterogeneous domains may be able to comment on the ability of cholesterol:ceramide mixtures to tune membrane biophysical properties.

## **Backbone structure is a secondary factor**

Ceramide and diacylglycerol are structurally similar; most notably, both possess a small polar headgroup. With their sphingosine backbone, ceramides are capable of both donating and accepting hydrogen bonds, in contrast to glycerides that can only accept hydrogen bonds. It is known that sphingolipid-rich condensed phases benefit from an inter- and intra-

molecular hydrogen bonding network that is coordinated by the C4 *trans*-double bond of the base.<sup>39,64–66</sup> This suggests that ceramide’s ability to form hydrogen bonds promotes the formation and stabilization of ceramide-rich platforms in sphingolipid mixtures.

From Figure 3, a comparison of C16:0-dag to C16:0-cer in the absence of sphingomyelin shows that clustering of DPPC is enhanced by chain-equivalent diacylglycerols compared to ceramides. However, the domain-enhancing feature offered by the diacylglycerol backbone is more than offset by the penalty of chain unsaturation (compare C18:1-dag to C18:1-cer in Fig. 3). This is in agreement with the findings of Megha and London, who showed that C16:0-dag is most efficient in displacing cholesterol from ordered bilayers due to its enhanced packing efficiency.<sup>50</sup> In addition, investigations by Sot et al. indicate that natural extracts of egg diacylglycerols destabilize sphingomyelin-rich phases, while egg ceramide is stabilizing.<sup>41</sup> In agreement with our data and the findings of others, it is likely that this observation is a result of the greater amount of saturated acyl chains in the ceramide extract (60 %), compared to the diacylglycerol extract (40 %), rather than a preference for one backbone structure over the other.

Maula et al. characterized the influence of phytosphingosine and 2'-hydroxyceramide species on phase separation. In a sphingolipid-rich system, they determined that the additional hydroxyl group increases domain stability due to greater hydrogen bonding. However, elimination of the C4 *trans*-double bond in phytosphingosine, and additional steric contributions from the -OH group, prevents the tight packing necessary for condensed phases.<sup>27</sup> Based on the structure of diacylglycerol, which is devoid of hydrogen bond donors, it is reasonable to attribute its affinity for glycerophospholipid phases largely to its structural similarity (and therefore favorability to pack) as compared to ceramide. Still, further investigations are warranted to explore the phase behavior of various diacylglycerol species in a sphingolipid-containing raft-mimicking composition to better compare the influence of hydrogen bonding and backbone structure.

## Summary and Conclusions

Using SANS from lipid vesicles that are models for membrane rafts, we observe differences in lipid clustering in the presence of ceramides and diacylglycerols of varying chain length and unsaturation. We draw two main conclusions from the data: 1) C16:0 and C18:0 ceramides stabilize ordered domains, in contrast to the destabilizing effect manifested by short (C6:0) or very long (C24:0) ceramides; and 2) monosaturated ceramides of any chain length destabilize lipid clustering. Although the molecular structure of the lipid backbone and its hydrogen bonding abilities further stabilize lipid domains, its role is of lesser consequence. Our findings can be explained by a competition between cholesterol and ceramide in seeking shelter from the aqueous phase, thus producing domains that bridge the biophysical properties of gel- and liquid-ordered phases.

## Experimental

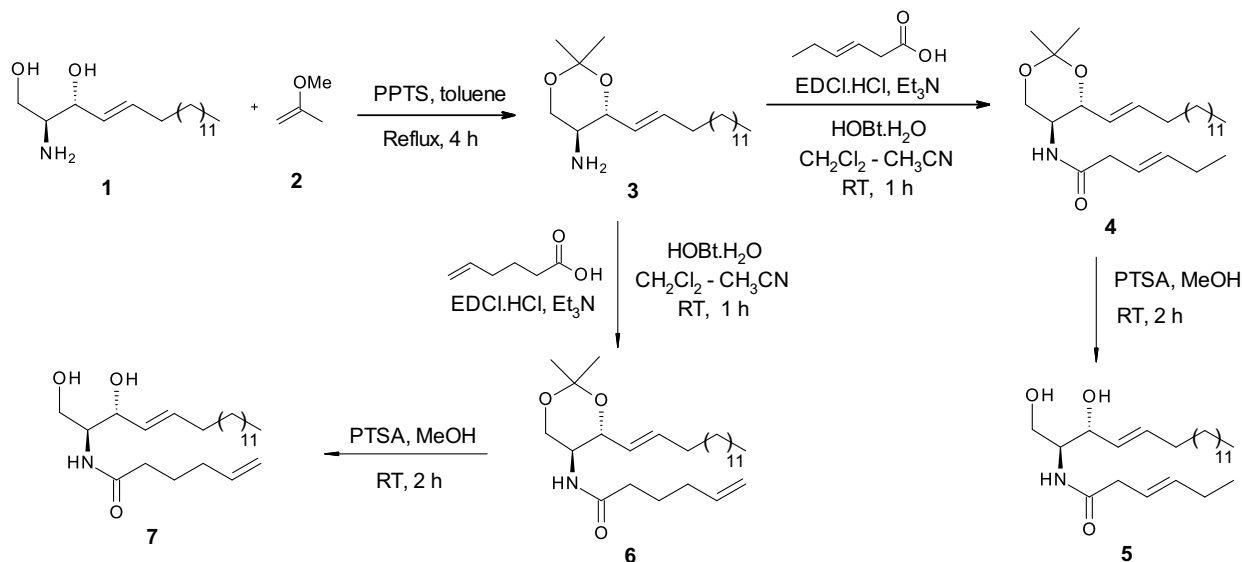
### Materials

Lipids and cholesterol were dissolved in HPLC-grade chloroform to a known concentration and stored at - 80 °C. Ultrapure H<sub>2</sub>O was obtained from a High-Q purification system (Wilmette, IL) and D<sub>2</sub>O (99.9%) was purchased from Cambridge Isotopes (Andover, MA). Cholesterol was from Nu-Chek Prep (Elysian, MN). 1,2-dipalmitoyl-*sn*-glycero-3-phosphocholine (DPPC), 1,2-dioleoyl-*sn*-glycero-3-phosphocholine (DOPC), 1,2-dipalmitoyl-*sn*-glycerol (C16:0-diacylglycerol, C16:0-dag), 1-palmitoyl-2-oleoyl-*sn*-glycerol (C18:1-diacylglycerol, C18:1-dag), *N*-hexanoyl-D-*erythro*-spingosine (C6:0-ceramide, C6:0-cer), *N*-lauroyl-D-*erythro*-spingosine (C12:0-ceramide, C12:0-cer), *N*-palmitoyl-D-*erythro*-spingosine (C16:0-ceramide, C16:0-cer), *N*-stearoyl-D-*erythro*-spingosine (C18:0-ceramide, C18:0-cer), *N*-oleoyl-D-*erythro*-spingosine (C18:1-ceramide, C18:1-cer), *N*-lignoceroyl-D-*erythro*-spingosine (C24:0-ceramide, C24:0-cer), and *N*-nervonoyl-D-*erythro*-spingosine (C24:1-ceramide, C24:1-cer) were purchased



from Avanti Polar Lipids (Alabaster, AL) and used as supplied.

*N*-hex-3-enoyl-*D*-*erythro*-sphingosine (**5**) and *N*-hex-5-enoyl-*D*-*erythro*-sphingosine (**7**) were prepared according to the synthetic steps outlined in Scheme 1 following literature methods.<sup>67,68</sup> Briefly, *D*-sphingosine (**1**) was converted to corresponding acetonide **3** by treating with 2-methoxy-1-propene (**2**) in the presence of a catalytic amount of pyridinium *p*-toluenesulfonate (PPTS) in refluxing toluene for 4 h.<sup>67</sup> The resulting *D*-sphingosine acetonide **3** and Et<sub>3</sub>N in CH<sub>3</sub>CN, on treatment with a solution of 1-hydroxybenzotriazole monohydrate (HOBt.H<sub>2</sub>O), *trans*-3-hexenoic acid or 5-hexenoic acid, and *N*-(3-dimethylaminopropyl)-*N*'-ethylcarbodiimide hydrochloride (EDCI.HCl) in CH<sub>2</sub>Cl<sub>2</sub> at room temperature for 1 h resulted in the corresponding acetonide protected C6-ceramide analogs **4** and **6** in 72 % and 75 % yields, respectively.<sup>68</sup> Compounds **4** and **6** on reaction with catalytic amount of *p*-toluenesulfonic acid (PTSA) in MeOH at room temperature for 2 h afforded the corresponding *N*-hex-3-enoyl-*D*-*erythro*-sphingosine (**5**) and *N*-hex-5-enoyl-*D*-*erythro*-sphingosine (**7**), respectively, in quantitative yields.<sup>67</sup> Both the compounds **5** and **7** were characterized on the basis of NMR and MS spectral data (DNS).



Scheme 1: Synthesis of C6:1-cer species.

## Preparation of LUVs for small-angle neutron scattering (SANS)

Large unilamellar vesicle (LUV) samples for SANS measurements were prepared as follows. Desired volumes of lipid and cholesterol stock solutions in chloroform were transferred to a glass vial using a glass syringe. Organic solvent was removed under a nitrogen stream with mild heating. Lipid films were then placed under vacuum for  $> 12$  h to remove trace solvent. Dry lipid films were hydrated with a 34.5 % (v/v)  $D_2O/H_2O$  mixture preheated to  $45\text{ }^\circ\text{C}$  and subsequently vortexed to generate multilamellar vesicles (MLVs). The MLV suspension was incubated at  $45\text{ }^\circ\text{C}$  for 1 h, followed by 5 freeze/thaw cycles between  $-80$  and  $45\text{ }^\circ\text{C}$ . Samples were then sonicated at  $60\text{ }^\circ\text{C}$  for 1 minute. Unilamellar liposomes were prepared using a miniextruder (Avanti Polar Lipids, Alabaster, AL) assembled with a single 50 nm diameter pore size polycarbonate filter and heated to  $45\text{ }^\circ\text{C}$ . Final sample concentrations were 10–20 mg/mL, allowing for sufficient water between vesicles to eliminate the interparticle structure factor. The resulting vesicles had an average diameter of  $90 \pm 10$  nm as determined by dynamic light scattering.

## SANS data collection

SANS experiments were conducted at the High Flux Isotope Reactor (HFIR) of the Oak Ridge National Laboratory (ORNL) using the CG-3 BioSANS instrument.<sup>69</sup> LUV suspensions were loaded into 1 mm path-length quartz cylindrical cells (Hellma USA, Plainview, NY) and mounted in a temperature-controlled holder with  $\pm 1\text{ }^\circ\text{C}$  accuracy. Scattered neutrons were counted with  $^3\text{He}$  linear position-sensitive detector tubes (GE Reuter Stokes, Twinsburg, OH) assembled to form a  $1 \times 1$  m ( $192 \times 256$  pixels) main detector, and a  $1 \times 0.8$  m ( $160 \times 256$  pixels) curved wide-angle “wing” detector. SANS data were collected with a single instrument configuration covering a total scattering range of  $0.003 < q < 0.8\text{ \AA}^{-1}$  using  $6\text{ \AA}$  wavelength neutrons (FWHM 15%) with the main and wing detectors at sample-to-detector distances of 15.5 m and 1.13 m, respectively. The tube closest to the beam of the wing detector was rotated out of the primary beam path by  $1.4^\circ$ . Neutron beam collimation

was defined by source and sample apertures (40 and 14 mm diameter, respectively) placed 17.5 m apart. No neutron guides or attenuators were used. The 2D data were reduced and combined using the Mantid software package.<sup>70</sup> Data were corrected for detector pixel sensitivity, dark current and sample transmission, as well as background scattering from water. Reduced 2D data sets were azimuthally averaged to obtain 1D SANS profiles of scattering intensity  $I$  vs. wavevector  $q$ , where  $q$  is a function of the neutron wavelength  $\lambda$  and scattering angle  $2\theta$  through the relationship  $q=4\pi \sin\theta/\lambda$ .

## SANS analysis

Data backgrounds were normalized by subtracting the slope of  $I(q)\times q^4$  vs.  $q^4$  for  $q > 0.6 \text{ \AA}^{-1}$  from the data to correct for sample-to-sample variation in the flat incoherent background.<sup>71,72</sup> Following Pencer et al.<sup>73</sup> data were then analyzed as model-independent quantities through the Porod invariant,  $Q$ :

$$Q = \int I(q)q^2 dq \quad (1)$$

To a first approximation,  $Q$  is related to the degree of phase separation and the difference in neutron scattering length density (i.e., the contrast) between the two phases as:

$$Q \approx a_d(1 - a_d)\Delta\rho^2, \quad (2)$$

where  $a_d$  and  $(1 - a_d)$  are the area fractions occupied by the domain and matrix phases, respectively, and  $\Delta\rho$  is the contrast between the phases. The resulting Porod invariants were normalized as a fraction of the invariant of the non-doped lipid mixture at 15 °C, where phase separation is understood to be most robust.

## **Conflict of Interest**

Penn State Research Foundation has licensed ceramide nanoliposome technology to Keystone Nano, Inc. (Pennsylvania) . M.K. is CTO and co-founder of Keystone Nano.

## **Contributions**

Conceived the project: M.K., J.K., F.A.H., T.G.D.. Designed the experiments: F.A.H., T.G.D., D.M., M.K., J.K.. Performed experiments: F.A.H., T.G.D., D.M., M.D., T.E.F.. Analyzed data: F.A.H., D.M., M.D.. Synthesized reagents: A.S.K., S.A., D.D.. Drafted the manuscript: M.D., D.M., F.A.H.. Revised the manuscript for intellectual content: M.D., D.M., F.A.H., M.K., J.K..

## **Acknowledgement**

F.A.H. is supported by NSF grant MCB-1817929 and NIH/National Institute of General Medical Sciences grant R01GM138887. D.M. is supported by Natural Science and Engineering Council of Canada (NSERC) funding reference number RGPIN-2018-04841. M.K. is supported by NIH grant 5P01 CA 171983-07. J.K. is supported by the Scientific User Facilities Division of the Department of Energy (DOE) Office of Science, sponsored by the Basic Energy Science (BES) Program, DOE Office of Science, under Contract No. DEAC05-00OR22725. A portion of this research used resources at the High Flux Isotope Reactor and the Biophysical Characterization Suite of the Shull Wollan Center, DOE Office of Science User Facilities operated by Oak Ridge National Laboratory.

## References

- (1) Ipsen, J.; Karlstrom, G.; Mouritsen, O.; Wennerstrom, H.; Zuckermann, M. Phase equilibria in the phosphatidylcholine-cholesterol system. *Biochim. Biophys. Acta* **1987**, *905*, 162–172.
- (2) Marsh, D. Cholesterol-induced fluid membrane domains: A compendium of lipid-raft ternary phase diagrams. *Biochim. Biophys. Acta* **2009**, *1788*, 2114–2123.
- (3) Heberle, F.; Feigenson, G. Phase separation in lipid membranes. *Cold Spring Harbor Perspectives in Biology* **2011**, *3*, a004630.
- (4) Simons, K.; Ikonen, E. Functional Rafts in Cell Membranes. *Nature* **1997**, *387*, 569–572.
- (5) Slotte, J. P. The importance of hydrogen bonding in sphingomyelin’s membrane interactions with co-lipids. *Biochimica et Biophysica Acta (BBA) - Biomembranes* **2016**, *1858*, 304–310.
- (6) Sodt, A.; Pastor, R.; Lyman, E. Hexagonal Substructure and Hydrogen Bonding in Liquid-Ordered Phases Containing Palmitoyl Sphingomyelin. *Biophys. J.* **2015**, *109*, 948–955.
- (7) Levental, I.; Levental, K.; Heberle, F. Lipid Rafts: Controversies Resolved, Mysteries Remain. *Trends in Cell Biology* **2020**, *30*, 341–353.
- (8) Feigenson, G. On the small size of liquid-disordered + liquid-ordered nanodomains. *Biochim. Biophys. Acta* **2021**, *1863*, 183685.
- (9) Veatch, S. From small fluctuations to large-scale phase separation: Lateral organization in model membranes containing cholesterol. *Sem. Cell & Dev. Biol.* **207**, *18*, 573–582.
- (10) Allender, D.; Giang, H.; Schick, M. Model Plasma Membrane Exhibits a Microemulsion in Both Leaves Providing a Foundation for ”Rafts”. *Biophys. J.* **2020**, *118*, 1019–1031.

- (11) Kolesnick, R. N.; Goñi, F. M.; Alonso, A. Compartmentalization of ceramide signaling: physical foundations and biological effects. *Journal of Cellular Physiology* **2000**, *184*, 285–300.
- (12) Wang, T.-Y.; Silvius, J. R. Sphingolipid Partitioning into Ordered Domains in Cholesterol-Free and Cholesterol-Containing Lipid Bilayers. *Biophysical Journal* **2003**, *84*, 367–378.
- (13) Huang, J.; Feigenson, G. W. A Microscopic Interaction Model of Maximum Solubility of Cholesterol in Lipid Bilayers. *Biophysical Journal* **1999**, *76*, 2142–2157.
- (14) Hannun, Y. A. Functions of Ceramide in Coordinating Cellular Responses to Stress. *Science* **1996**, *274*, 1855–1859.
- (15) Ali, M. R.; Cheng, K. H.; Huang, J. Ceramide Drives Cholesterol Out of the Ordered Lipid Bilayer Phase into the Crystal Phase in 1-Palmitoyl-2-oleoyl-sn-glycero-3-phosphocholine/Cholesterol/Ceramide Ternary Mixtures. *Biochemistry* **2006**, *45*, 12629–12638.
- (16) Goñi, F. M.; Alonso, A. Effects of ceramide and other simple sphingolipids on membrane lateral structure. *Biochimica et Biophysica Acta (BBA) - Biomembranes* **2009**, *1788*, 169–177.
- (17) Grassmé, H.; Jendrossek, V.; Bock, J.; Riehle, A.; Gulbins, E. Ceramide-Rich Membrane Rafts Mediate CD40 Clustering. *The Journal of Immunology* **2002**, *168*, 298–307.
- (18) Zhang, Y.; Li, X.; Becke, K. A.; Gulbins, E. Ceramide-enriched membrane domains – Structure and function. *Biochimica et Biophysica Acta (BBA) - Biomembranes* **2009**, *1788*, 178–183.
- (19) Cremesti, A. E.; Goñi, F. M.; Kolesnick, R. N. Role of sphingomyelinase and ceramide

- in modulating rafts: do biophysical properties determine biologic outcome? *FEBS Letters* **2002**, *531*, 47–53.
- (20) Kinnunen, P. K. J.; Kõiv, A.; Lehtonen, J. Y. A.; Rytömaa, M.; Mustonen, P. Lipid dynamics and peripheral interactions of proteins with membrane surfaces. *Chemistry and Physics of Lipids* **1994**, *73*, 181–207, Special Issue Functional Dynamics of Lipids in Biomembranes.
- (21) Mathias, S.; Peña, L. A.; Kolesnick, R. N. Signal transduction of stress via ceramide. *Biochemical Journal* **1998**, *335*, 465–480.
- (22) Stancevic, B.; Kolesnick, R. N. Ceramide-rich platforms in transmembrane signaling. *FEBS Letters* **2010**, *584*, 1728–1740, Frontiers in Membrane Biochemistry.
- (23) Li, Y. C.; Park, M. J.; Ye, S.-K.; Kim, C.-W.; Kim, Y.-N. Elevated Levels of Cholesterol-Rich Lipid Rafts in Cancer Cells Are Correlated with Apoptosis Sensitivity Induced by Cholesterol-Depleting Agents. *The American Journal of Pathology* **2006**, *168*, 1107–1118.
- (24) Huang, W.-C.; Chen, C.-L.; Lin, Y.-S.; Lin, C.-F. Apoptotic Sphingolipid Ceramide in Cancer Therapy. *Journal of Lipids* **2011**, *2011*, 1–15.
- (25) Pushkareva, M.; Obeid, L. M.; Hannun, Y. A. Ceramide: an endogenous regulator of apoptosis and growth suppression. *Immunology Today* **1995**, *16*, 294–297.
- (26) Laviad, E. L.; Albee, L.; Pankova-Kholmyansky, I.; Epstein, S.; Park, H.; Jr., A. H. M.; Futerman, A. H. Characterization of Ceramide Synthase 2 Tissue Distribution, Substrate Specificity, and Inhibition by Sphingosine-1-Phosphate. *Lipids and Lipoproteins* **2008**, *283*, 5677–5684.
- (27) Maula, T.; Al Sazzad, M.; Slotte, J. Influence of Hydroxylation, Chain Length, and

- Chain Unsaturation on Bilayer Properties of Ceramides. *Biophysical Journal* **2015**, *109*, 1639–1651.
- (28) Pinto, S. N.; Silva, L. C.; Futerman, A. H.; Preito, M. Effect of ceramide structure on membrane biophysical properties: the role of acyl chain length and unsaturation. *Biochimica et Biophysica Acta (BBA) - Biomembranes* **2011**, *1808*, 2753–2760.
- (29) Nybond, S.; Björkqvist, Y. J. E.; Ramstedt, B.; Slotte, J. P. Acyl chain length affects ceramide action on sterol/sphingomyelin-rich domains. *Biochimica et Biophysica Acta (BBA) - Biomembranes* **2005**, *1718*, 61–66.
- (30) Megha,; Sawatzki, P.; Kolter, T.; Bittman, R.; London, E. Effect of ceramide N-acyl chain and polar headgroup structure on the properties of ordered lipid domains (lipid rafts). *Biochimica et Biophysica Acta (BBA) - Biomembranes* **2007**, *1768*, 2205–2212.
- (31) Ackerman, D. G.; Heberle, F. A.; Feigenson, G. W. Limited Perturbation of a DPPC Bilayer by Fluorescent Lipid Probes: A Molecular Dynamics Study. *The Journal of Physical Chemistry B* **2013**, *117*, 4844–4852.
- (32) Pencer, J.; Mills, T. T.; Kucerka, N.; Nieh, M.-P.; Katsaras, J. *Lipid Rafts*; Springer, 2007; pp 231–244.
- (33) Heberle, F. A.; Petruzielo, R. S.; Pan, J.; Drazba, P.; Kučerka, N.; Standaert, R. F.; Feigenson, G. W.; Katsaras, J. Bilayer thickness mismatch controls domain size in model membranes. *Journal of the American Chemical Society* **2013**, *135*, 6853–6859.
- (34) Veatch, S. L.; Keller, S. L. Separation of Liquid Phases in Giant Vesicles of Ternary Mixtures of Phospholipids and Cholesterol. *Biophysical Journal* **2003**, *85*, 3074–3083.
- (35) Boulgaropoulos, B.; Rappolt, M.; Sartori, B.; Amenitsch, H.; Pabst, G. Lipid Sorting by Ceramide and the Consequences for Membrane Proteins. *Biophysical Journal* **2012**, *102*, 2031–2038.



- (36) Castro, B. M.; Silva, L. C.; Fedorov, A.; de Almeida, R. F.; Prieto, M. Cholesterol-rich Fluid Membranes Solubilize Ceramide Domains: Implications for the Structure and Dynamics of Mammalian Intracellular and Plasma Membranes. *Journal of Biological Chemistry* **2009**, *284*, 22978–22987.
- (37) Pinto, S. N.; Fernandes, F.; Fedorov, A.; Futerman, A. H.; Silva, L. C.; Prieto, M. A combined fluorescence spectroscopy, confocal and 2-photon microscopy approach to re-evaluate the properties of sphingolipid domains. *Biochimica et Biophysica Acta (BBA) - Biomembranes* **2013**, *1828*, 2099 – 2110.
- (38) Silva, L. C.; Futerman, A. H.; Prieto, M. Lipid Raft Composition Modulates Sphingomyelinase Activity and Ceramide-Induced Membrane Physical Alterations. *Biophysical Journal* **2009**, *96*, 3210–3222.
- (39) Jaikishan, S.; Slotte, J. P. Stabilization of sphingomyelin interactions by interfacial hydroxyls – A study of phytosphingomyelin properties. *Biochimica et Biophysica Acta (BBA) - Biomembranes* **2013**, *1828*, 391–397.
- (40) Pencer, J.; Mills, T.; Anghel, V.; Krueger, S.; Epand, R. M.; Katsaras, J. Detection of submicron-sized raft-like domains in membranes by small-angle neutron scattering. *European Physical Journal E* **2005**, *18*, 447–458.
- (41) Sot, J.; Ibarguren, M.; Busto, J. V.; Montes, L.-R.; Goñi, F. M.; Alonso, A. Cholesterol displacement by ceramide in sphingomyelin-containing liquid-ordered domains, and generation of gel regions in giant lipidic vesicles. *FEBS Letters* **2008**, *582*, 3230–3236.
- (42) Epand, R. M. Diacylglycerols, lysolecithin, or hydrocarbons markedly alter the bilayer to hexagonal phase transition temperature of phosphatidylethanolamines. *Biochemistry* **1985**, *24*, 7092–7095.

- (43) Marsh, D. Thermodynamic Analysis of Chain-Melting Transition Temperatures for Monounsaturated Phospholipid Membranes: Dependence on cis-Monoenoic Double Bond Position. *Biophysical Journal* **1999**, *77*, 953–963.
- (44) Dupuy, F. G.; Maggio, B. N-Acyl Chain in Ceramide and Sphingomyelin Determines Their Mixing Behavior, Phase State, and Surface Topography in Langmuir Films. *The Journal of Physical Chemistry B* **2014**, *118*, 7475–7487.
- (45) Pinto, S. N.; Silva, L. C.; de Almeida, R. F.; Preto, M. Membrane Domain Formation, Interdigitation, and Morphological Alterations Induced by the Very Long Chain Asymmetric C24:1 Ceramide. *Biophysical Journal* **2008**, *95*, 2867–2879.
- (46) Nyholm, T. K. M.; Grandell, P.-M.; Westerlund, B.; Slotte, J. P. Sterol affinity for bilayer membranes is affected by their ceramide content and the ceramide chain length. *Biochimica et Biophysica Acta (BBA) - Biomembranes* **2010**, *1798*, 1008–1013.
- (47) Carrer, D. C.; Maggio, B. Phase behavior and molecular interactions in mixtures of ceramide with dipalmitoylphosphatidylcholine. *Journal of Lipid Research* **1999**, *40*, 1987–1989.
- (48) Karttunen, M.; Haataja, M. P.; Säily, M.; Vattulainen, I.; Holopainen, J. M. Lipid Domain Morphologies in Phosphatidylcholines-Ceramide Monolayers. *Langmuir* **2009**, *25*, 4595–4600.
- (49) Silva, L. C.; de Almeida, R. F.; Castro, B. M.; Fedorov, A.; Prieto, M. Ceramide-Domain Formation and Collapse in Lipid Rafts: Membrane Reorganization by an Apoptotic Lipid. *Biophysical Journal* **2007**, *92*, 502–516.
- (50) Megha,; London, E. Ceramide Selectively Displaces Cholesterol from Ordered Lipid Domains (Rafts): Implications for Lipid Raft Structure and Function. *Journal of Biological Chemistry* **2004**, *279*, 9997–10004.

- (51) Alanko, S. M.; Halling, K. K.; Maunula, S.; Slotte, J. P.; Ramstedt, B. Displacement of sterols from sterol/sphingomyelin domains in fluid bilayer membranes by competing molecules. *Biochimica et Biophysica Acta (BBA) - Biomembranes* **2005**, *1715*, 111–121.
- (52) Levin, I. W.; Thompson, T. E.; Barenholz, Y.; Huang, C. Two types of hydrocarbon chain interdigitation in sphingomyelin bilayers. *Biochemistry* **1985**, *24*, 6282–6286.
- (53) Jiménez-Rojo, N.; García-Arribas, A. B.; Sot, J.; Alonso, A.; Goñi, F. M. Lipid bilayers containing sphingomyelins and ceramides of varying N-acyl lengths: A glimpse into sphingolipid complexity. *Biochimica et Biophysica Acta (BBA) - Biomembranes* **2014**, *1838*, 456–464.
- (54) Brown, G. C.; Nicholls, D. G.; Cooper, C. E.; Richter, C.; Ghafourifar, P. Ceramide induces cytochrome c release from isolated mitochondria. *Biochemical Society Symposia* **1999**, *66*, 27–31.
- (55) Ogretmen, B. Sphingolipid metabolism in cancer signalling and therapy. *Nat Rev Cancer* **2018**, *18*, 33–50.
- (56) Kester, M.; Bassler, J.; Fox, T. E.; Carter, C. J.; Davidson, J. A.; Parette, M. R. Pre-clinical development of a C6-ceramide NanoLiposome, a novel sphingolipid therapeutic. *Biological Chemistry* **2015**, *396*, 737–747.
- (57) Shaw, J.; Costa-Pinheiro, P.; Patterson, L.; Drews, K.; Spiegel, S.; Kester, M. In *Sphingolipids in Cancer*; Chalfant, C. E., Fisher, P. B., Eds.; Advances in Cancer Research; Academic Press, 2018; Vol. 140; pp 327–366.
- (58) Lange, Y.; Steck, T. L. Cholesterol homeostasis and the escape tendency (activity) of plasma membrane cholesterol. *Progress in Lipid Research* **2008**, *47*, 319–332.
- (59) Chiantia, S.; Kahya, N.; Ries, J.; Schwille, P. Effects of Ceramide on Liquid-Ordered

- Domains Investigated by Simultaneous AFM and FCS. *Biophysical Journal* **2006**, *90*, 4500–4508.
- (60) Busto, J. V.; Sot, J.; Requejo-Isidro, J.; Goñi, F. M.; Alonso, A. Cholesterol Displaces Palmitoylceramide from Its Tight Packing with Palmitoylsphingomyelin in the Absence of a Liquid-Disordered Phase. *Biophysical Journal* **2010**, *99*, 1119–1128.
- (61) Busto, J. V.; García-Arribas, A. B.; Sot, J.; Torrecillas, A.; Gómez-Fernández, J. C.; Goñi, F. M.; Alonso, A. Lamellar Gel ( $L_{\beta}$ ) Phases of Ternary Lipid Composition Containing Ceramide and Cholesterol. *Biophysical Journal* **2014**, *106*, 621–630.
- (62) García-Arribas, A. B.; Busto, J. V.; Alonso, A.; Goñi, F. M. Atomic Force Microscopy Characterization of Palmitoylceramide and Cholesterol Effects on Phospholipid Bilayers: A Topographic and Nanomechanical Study. *Langmuir* **2015**, *31*, 3135–3145, PMID: 25693914.
- (63) García-Arribas, A. B.; Alonso, A.; Goñi, F. M. Cholesterol interactions with ceramide and sphingomyelin. *Chemistry and Physics of Lipids* **2016**, *199*, 26–34, Properties and Functions of Cholesterol.
- (64) Li, X.-M.; Momsen, M. M.; Smaby, J. M.; Brockman, H. L.; Brown, R. E. Cholesterol Decreases the Interfacial Elasticity and Detergent Solubility of Sphingomyelins. *Biochemistry* **2001**, *40*, 5954–5963.
- (65) Löfgren, H.; Pascher, I. Molecular arrangements of sphingolipids. The monolayer behaviour of ceramides. *Chemistry and Physics of Lipids* **1977**, *20*, 273–284.
- (66) Brockman, H. L.; Momsen, M. M.; Brown, R. E.; He, L.; Chun, J.; Byun, H.-S.; Bittman, R. The 4,5-Double Bond of Ceramide Regulates Its Dipole Potential, Elastic Properties, and Packing Behavior. *Biophysical Journal* **2004**, *87*, 1722–1731.

- (67) Szulc, Z. M.; Bai, A.; Bielawski, J.; Mayroo, N.; Miller, D. E.; Gracz, H.; Hannun, Y. A.; Bielawska, A. Synthesis, NMR characterization and divergent biological actions of 2'-hydroxy-ceramide/dihydroceramide stereoisomers in MCF7 cells. *Bioorganic & Medicinal Chemistry* **2010**, *18*, 7565–7579.
- (68) Camacho, L.; Meca-Cortés, O.; Abad, J. L.; García, S.; Rubio, N.; Díaz, A.; Celià-Terrassa, T.; Cingolani, F.; Bermudo, R.; Fernández, P. L.; Blanco, J.; Delgado, A.; Casas, J.; Fabriàs, G.; Thomson, T. M. Acid ceramidase as a therapeutic target in metastatic prostate cancer. *Journal of Lipid Research* **2013**, *54*, 1207–1220.
- (69) Heller, W. T.; Cuneo, M.; Debeer-Schmitt, L.; Do, C.; He, L.; Heroux, L.; Littrell, K.; Pingali, S. V.; Qian, S.; Stanley, C.; Urban, V. S.; Wu, B.; Bras, W. The suite of small-angle neutron scattering instruments at Oak Ridge National Laboratory. *Journal of Applied Crystallography* **2018**, *51*, 242–248.
- (70) Arnold, O. et al. Mantid - Data analysis and visualization package for neutron scattering and  $\mu$  SR experiments. *Nuclear Instruments and Methods in Physics Research, Section A: Accelerators, Spectrometers, Detectors and Associated Equipment* **2014**, *764*, 156–166.
- (71) Porod, G. Die Röntgenkleinwinkelstreuung von dichtgepackten kolloiden Systemen. *Kolloid-Zeitschrift* **1951**, *124*, 83–114.
- (72) Alava, C.; Arrighi, V.; Cameron, J. D.; Cowie, J. M. G.; Moeller, A.; Triolo, A.; Vaqueiro, P. SANS studies of solutions and molecular composites prepared from cellulose tricarbonyl. *Applied Physics A: Materials Science and Processing* **2002**, *74*, 472–475.
- (73) Pencer, J.; Anghel, V. N.; Kučerka, N.; Katsaras, J. Scattering from laterally heterogeneous vesicles. I. Model-independent analysis. *Journal of Applied Crystallography* **2006**, *39*, 791–796.

## Graphical TOC Entry

Some journals require a graphical entry for the Table of Contents. This should be laid out “print ready” so that the sizing of the text is correct.

Inside the tocentry environment, the font used is Helvetica 8 pt, as required by *Journal of the American Chemical Society*.

The surrounding frame is 9 cm by 3.5 cm, which is the maximum permitted for *Journal of the American Chemical Society* graphical table of content entries. The box will not resize if the content is too big: instead it will overflow the edge of the box.

This box and the associated title will always be printed on a separate page at the end of the document.